

Spatial interactions in a modified Daisyworld model: Heat diffusivity and greenhouse effectsT. Alberti,^{1,*} L. Primavera,¹ A. Vecchio,^{2,3} F. Lepreti,^{1,4} and V. Carbone^{1,5}¹*Dipartimento di Fisica, Università della Calabria, Ponte P. Bucci Cubo 31C, 87036 Rende (CS), Italy*²*INGV Istituto Nazionale di Geofisica e Vulcanologia, Sede di Cosenza, Rende (CS), Italy*³*LESIA-Observatoire de Paris, 5 place Jules Janssen, 92190 Meudon, France*⁴*CNISM Unità di Cosenza, Ponte P. Bucci 31C, 87036 Rende (CS), Italy*⁵*ISAC/CNR Lamezia Terme (CZ), Italy*

(Received 26 November 2014; revised manuscript received 19 October 2015; published 23 November 2015)

In this work we investigate a modified version of the Daisyworld model, originally introduced by Lovelock and Watson to describe in a simple way the interactions between an Earth-like planet, its biosphere, and the incoming solar radiation. Here a spatial dependency on latitude is included, and both a variable heat diffusivity along latitudes and a simple greenhouse effect description are introduced in the model. We show that the spatial interactions between the variables of the system can locally stabilize the coexistence of the two vegetation types. The feedback on albedo is able to generate equilibrium solutions which can efficiently self-regulate the planet climate, even for values of the solar luminosity relatively far from the current Earth conditions.

DOI: [10.1103/PhysRevE.92.052717](https://doi.org/10.1103/PhysRevE.92.052717)

PACS number(s): 87.90.+y, 92.70.Np, 91.62.Xy, 92.70.Gt

I. INTRODUCTION

The comprehension of the interaction mechanisms between the Earth, its biosphere, and the solar radiation, driving global climate changes, represents a complex and still open problem that requires a deeper understanding. Advanced climate simulations can provide some insight into the complexity of the system, even though the existence of many forcings and parameters that are not easy to control represent a considerable difficulty. As an alternative approach, simple models can sometimes capture the fundamental dynamical mechanisms of the system. The so-called Daisyworld model, originally developed by Lovelock and Watson and [1–3], is one of the most famous examples. The model is based on a hypothetical planet, like the Earth, which receives the radiant energy coming from a Sun-like star, and is populated by two kinds of identical plants differing in their color: white daisies reflecting light and black daisies absorbing light. The interactions and feedbacks between the collective biota of the planet and the incoming radiation form a self-regulating system where the conditions for life are maintained. For a more complete review, see Ref. [3].

The original Daisyworld is a zero dimensional model with no explicit representation of space and negligible atmospheric greenhouse effect. Solar radiation is assumed to be distributed evenly over the planet and the two daisy populations receive the same amount of radiation but, because of their contrasting albedos, local microclimates with different temperatures are generated. Results show that the surface temperature of the Daisyworld remains almost constant for a broad range of the solar constant. On the other hand, the fractions of daisies covering the planet depend on the solar input.

The first model has been revisited and refined in several papers [4]. However, only a few authors (see, e.g. [3]) investigated the spatial dependence of the model to study the impact of different vegetation patterns and the role of feedbacks in desert formation [3,5–9]. When the heat diffusion

is constant, and the temperature does not continuously change with latitude, the coexistence equilibrium of the two daisy types is destabilized. Thus a striped pattern, consisting of black and white daisy bands, related to a Turing-like process [4] which causes the uniform equilibrium state to be unstable to nonconstant perturbations, emerges as an unrealistic aspect [7,8].

In this work we present a version of the Daisyworld model which includes spatial dependency, variable heat diffusivity, and the greenhouse effect by means of a grayness function. It is shown that the model exhibits significant features, including a destabilization effect due to heat diffusion, a global heating process driven by the greenhouse effect, and a remarkable dependence on the initial conditions of both daisy coverage and temperature profile.

II. MODEL

According to the Daisyworld model [1,2], the evolution of white and black daisies is described by the logistic equations

$$\frac{d\alpha_w}{dt} = \alpha_w(x\beta_w - \gamma), \quad (1)$$

$$\frac{d\alpha_b}{dt} = \alpha_b(x\beta_b - \gamma), \quad (2)$$

where α_w and α_b are the fractions of surface covered by white and black daisies, respectively, $x = 1 - \alpha_w - \alpha_b$ is the fraction of surface of fertile ground not covered by daisies, β_w and β_b are the growth rates of white and black daisies, and γ is the death rate per unit of time. The parameter γ is fixed to 0.3 [1,2,8], while the growth rate of the daisies is assumed to be

$$\beta_\ell(T) = \begin{cases} 1 - \delta(T_e - T_\ell(T))^2 & |T_e - T_\ell(T)| \leq \delta^{-\frac{1}{2}}, \\ 0 & \text{otherwise,} \end{cases} \quad (3)$$

where the subscript ℓ denotes the species (either w or b), $\delta = 0.003265$, which corresponds to a growth interval $5^\circ\text{C} \leq T_\ell(T) \leq 40^\circ\text{C}$, T is the surface temperature, and T_ℓ represents the local temperature of each daisy species [1,2].

*tommaso.alberti@unical.it

The maximum value $\beta = 1$ is reached when the local temperature is equal to the effective temperature $T_e = 22.5^\circ\text{C}$. In a simple linear approximation [1,3], the local temperature depends on the albedo of the Daisyworld surface A and on T as $T_\ell = q(A(\theta, t) - A_\ell) + T(\theta, t)$, where q is a measure of local heat diffusion, assumed to be $q = 20\text{ K}$ according to the original model [1,2]. The albedo A of the planet depends on the coverage in the following way:

$$A = \alpha_w A_w + \alpha_b A_b, \quad (4)$$

where A_w and A_b represent the albedos of the two species, which, in the original papers [1,2], are set to $A_w = 0.75$ and $A_b = 0.25$, respectively (here we assume that there is no bare ground). The temperature at which the planet radiates is calculated from the equilibrium between absorbed and emitted radiation, $\sigma T^4 = SL(1 - A)$, where σ is the Stefan's constant, S is the solar constant, and L is a dimensionless parameter that describes the luminosity of the Daisyworld's sun ($L = 1$ for the present Earth). Numerical simulations show that the system settles down towards an equilibrium solution for a wide range of values of the luminosity $0.5 \leq L \leq 1.5$ [1,8].

The development of a Daisyworld model with spatial dependence gives room for (1) the possibility of inhomogeneous solar forcing in a spherical planet, with explicit differences between poles and equator, and (2) the direct use of the heat diffusion equation, so that the radiative equilibrium equation can be replaced by

$$\rho c_p \frac{\partial T}{\partial t} = (1 - A)R(\theta) - \sigma T^4 + \nabla \cdot [\chi(\nabla T)], \quad (5)$$

where c_p and χ are the heat capacity and the conductivity of the Earth, ρ is the mass density of the atmosphere, and R describes the incident radiation. As a first approach, to describe a spherical planet, we assume that the temperature $T(\theta, t)$ and the surface coverage depend only on time and on latitude θ ($-90^\circ \leq \theta \leq 90^\circ$). The inhomogeneous solar forcing is taken into account by introducing the following simple functional form for R :

$$R(\theta) = \frac{4}{\pi} SL \cos(\theta), \quad (6)$$

where we used $S = 1366\text{ W m}^2$, which is a typical value for the solar constant. Since one of the weak points of the classical Daisyworld model is the absence of the atmosphere and the contribution of greenhouse gases, playing an important role in an Earth-like planet, is not included, we introduce, as a further step, the greenhouse effect in the model. This effect can be described by introducing a grayness function $g(T)$ [10,11] in Eq. (5), through the term $g(T)\sigma T^4$. As a final step, we consider a latitude dependence of the Earth's conductivity, $\chi = \chi(\theta)$. Both functions $g(T)$ and $\chi(\theta)$ require to be properly modeled.

By adding these terms and using spherical coordinates, the modified Daisyworld model is described by the following set of equations:

$$\frac{\partial \alpha_w}{\partial t} = \alpha_w [(1 - \alpha_w - \alpha_b)\beta_w(T) - \gamma], \quad (7)$$

$$\frac{\partial \alpha_b}{\partial t} = \alpha_b [(1 - \alpha_w - \alpha_b)\beta_b(T) - \gamma], \quad (8)$$

$$\begin{aligned} \frac{\partial T}{\partial t} = & \frac{1}{\rho c_p} [1 - A(\theta, t)]R(\theta) - \frac{\sigma}{\rho c_p} g(T)T^4 \\ & + \frac{1}{r_E^2 \cos \theta} \frac{\partial}{\partial \theta} \left[\kappa(\theta) \cos \theta \frac{\partial T}{\partial \theta} \right], \end{aligned} \quad (9)$$

where $\alpha_{w,b}$ are functions of both latitude and time, $\kappa(\theta) = \chi(\theta)/\rho c_p$, and $r_E \simeq 6.37 \times 10^8\text{ cm}$ is the Earth's radius. We use the expression of the Laplace operator in spherical coordinates, taking into account that, in our case, $-90^\circ \leq \theta \leq 90^\circ$.

III. STABILITY ANALYSIS

To investigate the role of the greenhouse effect into the energy budget between emitted and absorbed radiation in the Daisyworld we performed the stability analysis on the model described by Eqs. (7)–(9). By following the approach of Refs. [7,8], these equations can be written in a compact form as

$$\frac{\partial u}{\partial t} = u\phi(u, v, T), \quad (10)$$

$$\frac{\partial v}{\partial t} = v\psi(u, v, T), \quad (11)$$

$$\frac{\partial T}{\partial t} = h(u, v, T) + \frac{1}{r_E^2 \cos \theta} \frac{\partial}{\partial \theta} \left[\kappa(\theta) \cos \theta \frac{\partial T}{\partial \theta} \right], \quad (12)$$

where $u \doteq \alpha_w$, $v \doteq \alpha_b$, and

$$\phi(u, v, T) = (1 - \alpha_w - \alpha_b)\beta_w(T) - \gamma,$$

$$\psi(u, v, T) = (1 - \alpha_w - \alpha_b)\beta_b(T) - \gamma,$$

$$h(u, v, T) = \frac{1}{\rho c_p} \{ [1 - A(\theta, t)]R(\theta) - \sigma g(T)T^4 \}.$$

Note that in Eq. (12) the greenhouse term is included in $h(u, v, T)$.

In the following subsections, we discuss the stability of the system for three different cases: (A) without greenhouse effect and diffusion; (B) with greenhouse effect and no diffusion; (C) with both greenhouse effect and diffusion.

A. No greenhouse effect [$g(T) = 1$] and no diffusion [$\kappa(\theta) = 0$]

For fixed T , four equilibrium points $P_i = (u, v)$, corresponding to four different physical situations, are obtained as follows.

(i) $P_1 = (0, 0) \Rightarrow$ No daisies. Unstable equilibrium point.

(ii) $P_2 = (\bar{u}, 0) \Rightarrow$ White daisies only. This is a stable equilibrium point if $T \geq 292.13\text{ K}$.

(iii) $P_3 = (0, \bar{v}) \Rightarrow$ Black daisies only. This is a stable equilibrium point if $T \leq 298.87\text{ K}$.

(iv) $P_4 = (u_c, v_c) \Rightarrow$ Coexistence of white and black daisies. This is a stable equilibrium point if $292.13\text{ K} < T < 298.87\text{ K}$.

This case was previously studied in Refs. [7,8].

B. Greenhouse effect [$g(T) \neq 1$] and no diffusion [$\kappa(\theta) = 0$]

Let's now study the effects of the greenhouse by choosing a grayness function

$$g(T) = 1 - \frac{1}{2} \tanh\left(\frac{T}{T_0}\right)^6. \quad (13)$$

This functional form of $g(T)$, with $T_0^{-6} = 1.9 \times 10^{-15} \text{ K}^{-6}$, takes into account the infrared emission due to the Earth's surface which is assumed to increase with the surface temperature T and which implies a relaxation of the blackbody radiation hypothesis [11].

By following the standard equilibrium point analysis, we linearized Eqs. (10)–(12) and studied the sign of the eigenvalues of the associated Jacobian matrix. We thus write down the variables as the sum of mean quantities (u_c, v_c, T_c) and small amplitude perturbations (u', v', T')

$$u = u_c + u', \quad (14)$$

$$v = v_c + v', \quad (15)$$

$$T = T_c + T', \quad (16)$$

with $(u', v', T') \ll (u_c, v_c, T_c)$ and $P_c = (u_c, v_c, T_c)$ is the equilibrium point associated with the coexistence solution. After linearizing Eqs. (10)–(12), the Jacobian matrix (J) at the equilibrium point P_c

$$J(P_c) = \begin{bmatrix} \phi(P_c) + u_c \phi_u(P_c) & u_c \phi_v(P_c) & u_c \phi_T(P_c) \\ v_c \psi_u(P_c) & \psi(P_c) + v_c \psi_v(P_c) & v_c \psi_T(P_c) \\ h_u(P_c) & h_v(P_c) & h_T(P_c) \end{bmatrix} \quad (17)$$

has been evaluated. In the Jacobian calculation we use the condition $\phi(P_c) = \psi(P_c) = 0$, satisfied by the coexistence solution [7,8]. The stability of the system is defined by the properties of the J eigenvalues obtained from the solutions of the equation $E(\lambda) = 0$, where $E(\lambda)$ is defined as

$$E(\lambda) = \begin{vmatrix} u_c \phi_u - \lambda & u_c \phi_v & u_c \phi_T \\ v_c \psi_u & v_c \psi_v - \lambda & v_c \psi_T \\ h_u & h_v & h_T - \lambda \end{vmatrix}, \quad (18)$$

in which the dependence of ϕ , ψ , and h on P_c has been omitted.

The zeros of $E(\lambda)$ are obtained by expanding with respect to the third column:

$$E(\lambda) = (h_T - \lambda) \begin{vmatrix} u_c \phi_u - \lambda & u_c \phi_v \\ v_c \psi_u & v_c \psi_v - \lambda \end{vmatrix} - v_c \psi_T \begin{vmatrix} u_c \phi_u - \lambda & u_c \phi_v \\ h_u & h_v \end{vmatrix} + u_c \phi_T \begin{vmatrix} v_c \psi_u & v_c \psi_v - \lambda \\ h_u & h_v \end{vmatrix}. \quad (19)$$

Since the derivatives of the functions ϕ and ψ are of order δ and $\delta \ll 1$ [see Eq. (3)], the eigenvalues can be written as

$$\lambda_1 = h_T + O(\delta), \quad (20)$$

$$\lambda_2 = -b + O(\delta), \quad (21)$$

$$\lambda_3 = c\delta + O(\delta^2), \quad (22)$$

where b and c are two constants with $b > 0$ and $c < 0$ [8]. The system has two negative eigenvalues (λ_2 and λ_3); therefore, the stability only depends on the sign of λ_1 which is related to the sign of h_T . A calculation shows that

$$h_T = \frac{1}{\rho c_p} \left\{ -\sigma T^3 \left[\frac{dg}{dT} T + 4g(T) \right] + \frac{R}{5} \right\}. \quad (23)$$

By defining $\tilde{h}_T = (\rho c_p h_T)/(\sigma T_0^3)$, $\zeta = R/(5\sigma T_0^3)$ and setting $x = (T/T_0)^3$, we obtain

$$\tilde{h}_T = -x[-3x^2 \cosh^{-2}(x^2) + 4 - 2 \tanh(x^2)] + \zeta, \quad (24)$$

and, as a consequence,

$$\tilde{h}_T < 0 \Rightarrow x > x_0 = 0.149. \quad (25)$$

This condition sets a critical value of temperature below which the coexistence solution becomes unstable. According to our choice $T_0 = 284.15 \text{ K}$, the coexistence solution is stable if $T > 150.65 \text{ K}$, but considering that the coexistence solution exists if $292.13 \text{ K} < T < 298.87 \text{ K}$, the grayness function does not destabilize it.

C. Greenhouse effect [$g(T) \neq 1$] and constant diffusion [$\kappa(\theta) = \text{const}$]

The coexistence solution can be destabilized only in the presence of a mechanism, such as the diffusion process, which is able to set one of the three eigenvalues greater than zero. The role of the diffusivity can be evaluated through the stability analysis on Eqs. (10)–(12), in which we consider a simplified diffusion term [8]

$$\frac{\partial u}{\partial t} = u\phi(u, v, T), \quad (26)$$

$$\frac{\partial v}{\partial t} = v\psi(u, v, T), \quad (27)$$

$$\frac{\partial T}{\partial t} = h(u, v, T) + D \frac{\partial^2 T}{\partial \theta^2}, \quad (28)$$

where we set $\kappa(\theta)/r_E^2 = D = \text{const}$ and where we neglect the term of the Laplace operator which is proportional to the temperature gradient [7,8]. By linearizing the system and by choosing a temperature perturbation in the form $\delta T \propto e^{ik_\theta \theta}$, the eigenvalues of the Jacobian matrix can be obtained as the zeros of the function $E(\lambda, Dk_\theta)$, whose functional form is the same as that of Eq. (18) with $h_T - Dk_\theta^2 - \lambda$ replacing $h_T - \lambda$. In this particular case, the eigenvalues become

$$\lambda_1 = h_T - Dk_\theta^2 + O(\delta), \quad (29)$$

$$\lambda_2 = -b - k_\theta^2 + O(\delta), \quad (30)$$

$$\lambda_3 = c(Dk_\theta)\delta + O(\delta^2), \quad (31)$$

where $c(Dk_\theta)$ is a function of Dk_θ [7,8]. It is possible to note that the eigenvalues λ_1 and λ_2 are negative, while the sign of the third eigenvalue λ_3 can change. Following [7,8], it can be shown that the sign of λ_3 depends on Dk_θ and the first unstable mode is given by $Dk_\theta = 8$. This critical parameter, higher than the corresponding parameter evaluated in Ref. [7] where no greenhouse term was included, is a measure of the effect of the diffusion and the grayness function on the stability of the coexistence solution. In the Daisyworld model we developed, the destabilization process is modified by the concurrent effect of both the greenhouse effect, modeled through the grayness function, and the latitudinal diffusion process.

IV. NUMERICAL RESULTS

Equations (7)–(9), with the condition (4), have been solved numerically by using a second order Runge-Kutta scheme for time integration and spectral methods for integration on latitude θ . The poles ($\theta = \pm 90^\circ$) are singular points for the Laplace operator in spherical coordinates. At the poles we assume a free-flux boundary condition, corresponding to zero derivatives for all the variables. In this way the continuity of the Laplacian in these points is ensured, providing that suitable parity boundary conditions are imposed.

In order to recover the classical results, a first set of solutions was calculated by imposing a constant normalized grayness function $g(T) = 1$ and normalized heat conductivity $\kappa(\theta) = 1$ for each θ . In this case, the initial condition for T is set to $T(\theta, 0) = -20 + 40L \cos^2(\theta)$, and the initial coverages are constant $\alpha_w(\theta, 0) = \alpha_b(\theta, 0) = 0.5$ over θ . Figure 1 shows the equilibrium values of temperature and daisy coverage, as functions of the variable θ , for three different values of L . The equilibrium temperature profile is the expected one, namely a bell shaped curve peaked at the equator ($\theta = 0^\circ$). The increase or decrease of L corresponds to a global enhancement or decrease of temperature [1,8]. When L assumes the lowest value $L = 0.5$, corresponding to half the present solar luminosity, the planet becomes completely frozen, the highest temperature being $T(\theta = 0^\circ) \simeq -120^\circ\text{C}$. Conversely, when the value of L is the highest, $L = 1.5$, the planet is extremely hot, the lowest temperature being $T(\theta = \pm 90^\circ) \simeq 100^\circ\text{C}$. The behavior of daisies coverage is shown in the middle and lower panels of Fig. 1. An increase of luminosity L produces an increase of the planetary surface covered by black daisies and a decrease of the area covered by white daisies. This behavior indicates that black daisies withstand high temperatures, while the growth of white flowers is favored by low temperatures. By changing L in a continuous way the contour plots of equilibrium temperature and daisy coverages as functions of latitude and luminosity L can be built (Fig. 2). Numerical results show that, after some time steps, the system settles down to an equilibrium state where the various quantities do not change anymore in time. Figure 2 shows that global temperature increases with luminosity and the planet is almost completely frozen for $L \lesssim 1$. The daisy coverage is also related to L with an enhancement of black daisies for high values of luminosity.

In the classical Daisyworld model the heat conductivity is assumed to be constant, while actually it depends on temperature. In our model we use a heat conductivity peaked at

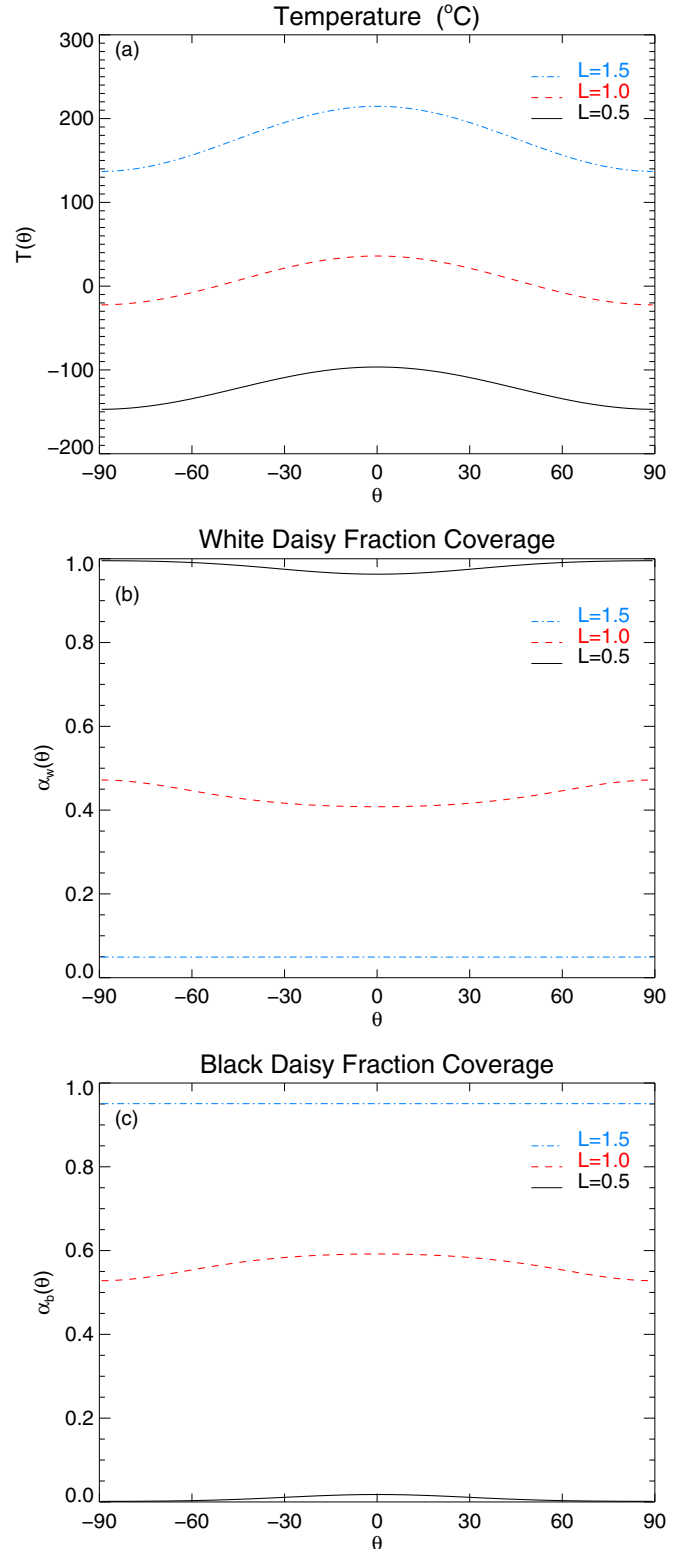


FIG. 1. (Color online) Stationary solutions for (a) temperature $T(\theta)$, (b) white daisy population $\alpha_w(\theta)$, and (c) black daisy population $\alpha_b(\theta)$, as a function of latitude, from the numerical solution of Eq. (9), using $\kappa(\theta) = 1$, $g(T) = 1$, and three different values of the parameter L .

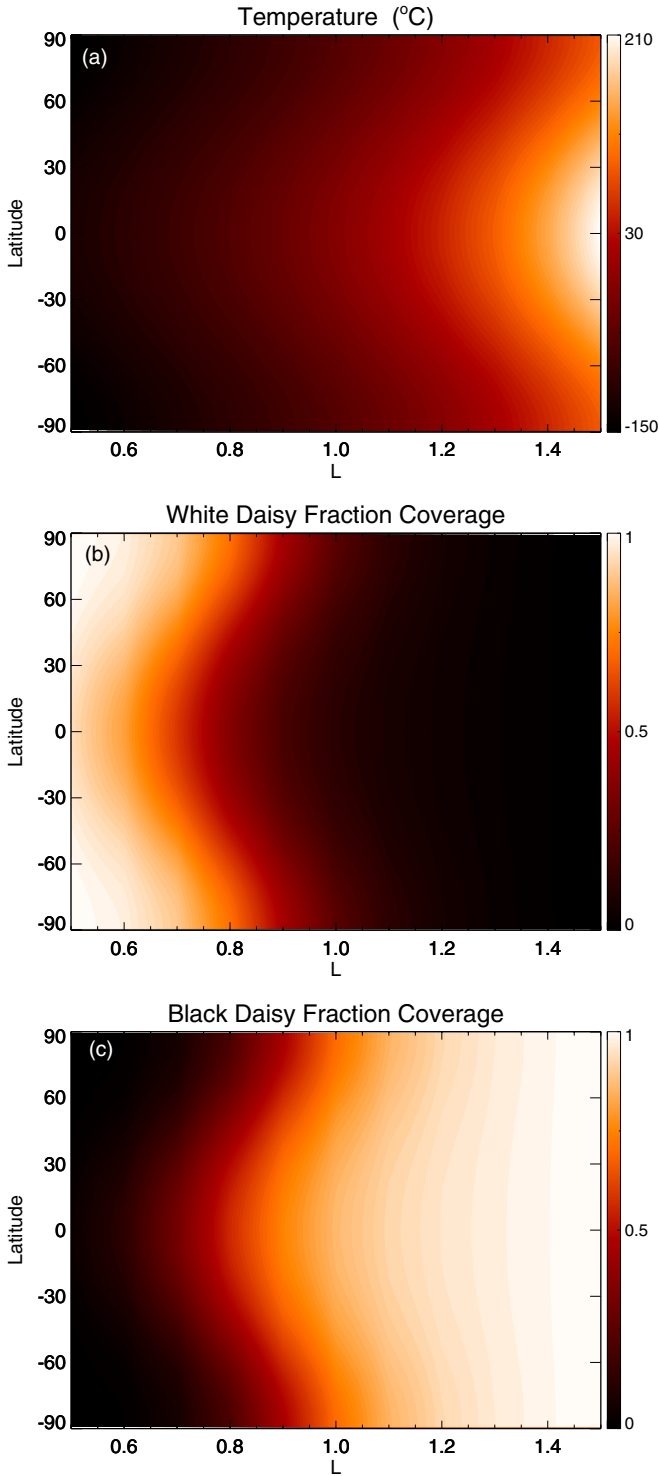


FIG. 2. (Color online) Contour plots of the stationary solutions for (a) $T(\theta)$, (b) white daisy population $\alpha_w(\theta)$, and (c) black daisy population $\alpha_b(\theta)$, in the plane (L, θ) using $\kappa(\theta) = 1$ and $g(T) = 1$.

the equator and decreasing toward the poles, where it vanishes. This is modeled by using the following functional form:

$$\kappa(\theta) = \frac{1 + \cos(2\theta)}{2}, \quad (32)$$

which is symmetrical around $\theta = 0^\circ$. Results obtained by using Eq. (32) in Eq. (9) and with the same initial conditions as in previous case are shown in Figs. 3 and 4. First of all, we note that the temperature variations with L are smaller with respect to the previous case in which the thermal diffusivity was not included. Moreover, as shown by middle and lower panels of Fig. 4, heat diffusion produces, for extreme values of L , larger differences in daisy fraction between polar and equatorial regions. Indeed, for low L values, the black daisy coverage in the region $0^\circ < \theta \lesssim 40^\circ$ is higher than in the previous case and for all L values the polar areas ($|\theta| \gtrsim 60^\circ$) are mainly populated by white daisies. A particular characteristic is the presence of an asymmetry in daisy coverage profiles not observed in the previous case. This behavior is due to the Laplace operator which consists in two different terms: the first one is symmetric, while the second one is not, since it is proportional to the derivative of $\kappa(\theta)$ with respect to θ .

A crucial point that we want to study is the effect of the atmospheric greenhouse gases on the planetary energy budget. This is done by using the grayness function given in Eq. (13) into the heat equation. The results obtained with the greenhouse effect are shown in Figs. 5 and 6. When both greenhouse and diffusion terms are considered, the global equilibrium temperature is changed again. A general increase of the temperature is found with respect to the previous case, where only the heat diffusion was added to the original Daisyworld model. The greenhouse effect acts as a self-regulating process for the planet climate. The temperature variations show a typical range between -30°C (at the poles, for $L = 0.5$) and 110°C (at the equator, for $L = 1.5$). Figure 6 (middle and lower panel) show that there is an increase of black daisy coverage in the region $|\theta| \lesssim 40^\circ$ for $L > 1$. With the inclusion of the greenhouse effect the symmetry is recovered because, when the grayness function is considered, the diffusion and the Stefan-Boltzmann terms are of the same order of magnitude; the symmetry with respect to θ is thus restored because these two terms are opposite in sign.

The equilibrium vegetation profiles depend also, to some extent, on the initial conditions of daisy coverage. In particular, by changing the initial conditions, the temperature profile remains unchanged, while the surface coverage gives rise to different dynamics. This can be seen in Figs. 7 and 8, which show the results obtained by leaving the initial temperature profile unchanged and choosing the initial daisy coverage in the form

$$\alpha_w(\theta, 0) = \begin{cases} \left| \frac{\theta}{\pi} \right| & \text{if } |\theta| < 85^\circ, \\ 0.5 & \text{otherwise,} \end{cases} \quad (33)$$

$$\alpha_b(\theta, 0) = 0.5 - \alpha_w(\theta, 0).$$

We note that, due to the chosen symmetry conditions, the time evolution of the fraction coverage for both species is symmetric but shows different shapes and values with respect to the previous case.

Another issue which is worth investigating is the occurrence of multiple steady states and the stability of the system with respect to the presence of perturbations in the initial temperature profile. To this aim, we numerically solved Eqs. (7)–(9) for a set of initial conditions such as $T(\theta, 0) = 295.5 + \cos(k_\theta)$, $\alpha_w(\theta, 0) = \frac{T(\theta, 0) - 292.13}{10}$, and $\alpha_b(\theta, 0) = \frac{298.87 - T(\theta, 0)}{10}$, where

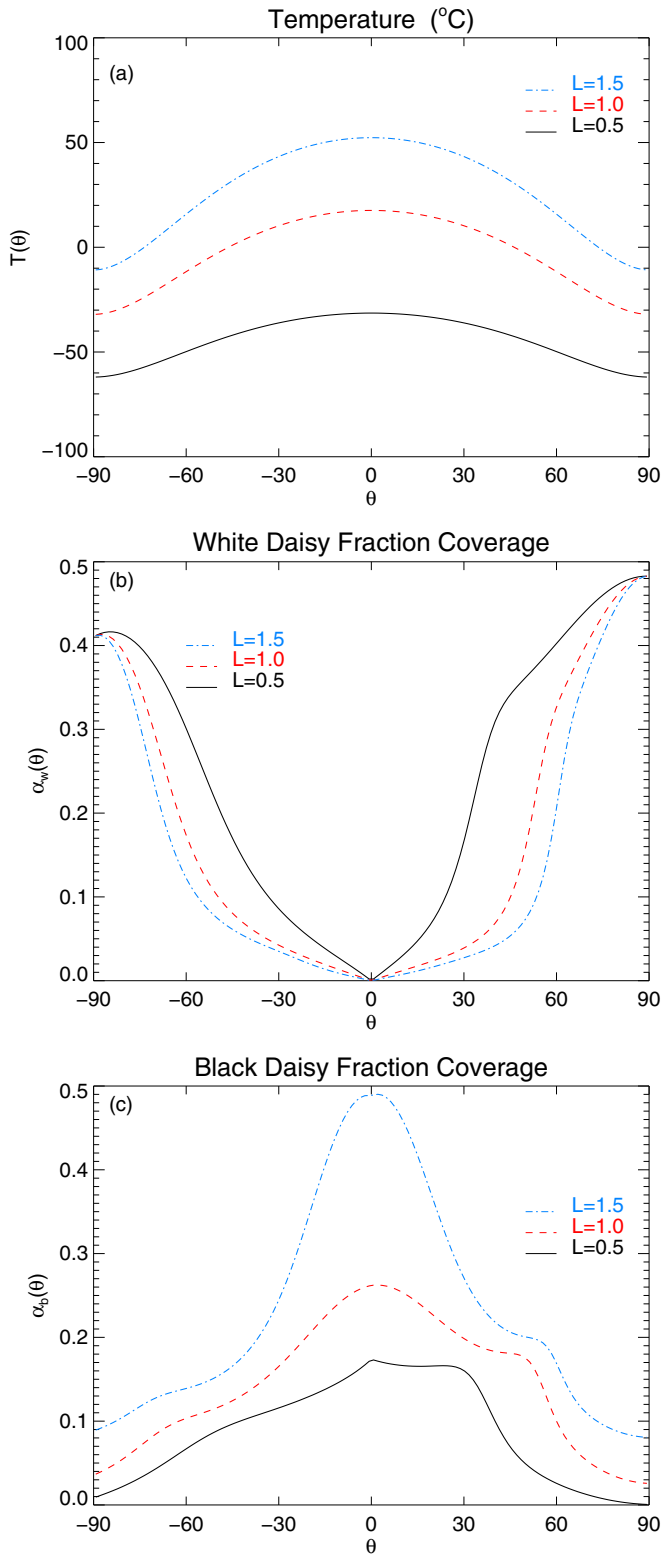


FIG. 3. (Color online) Stationary solutions for (a) temperature $T(\theta)$, (b) white daisy population $\alpha_w(\theta)$, and (c) black daisy population $\alpha_b(\theta)$, as a function of latitude, by numerical solution of Eq. (9), using the profile (32) for $\kappa(\theta)$ and $g(T) = 1$, and three different values of the parameter L .

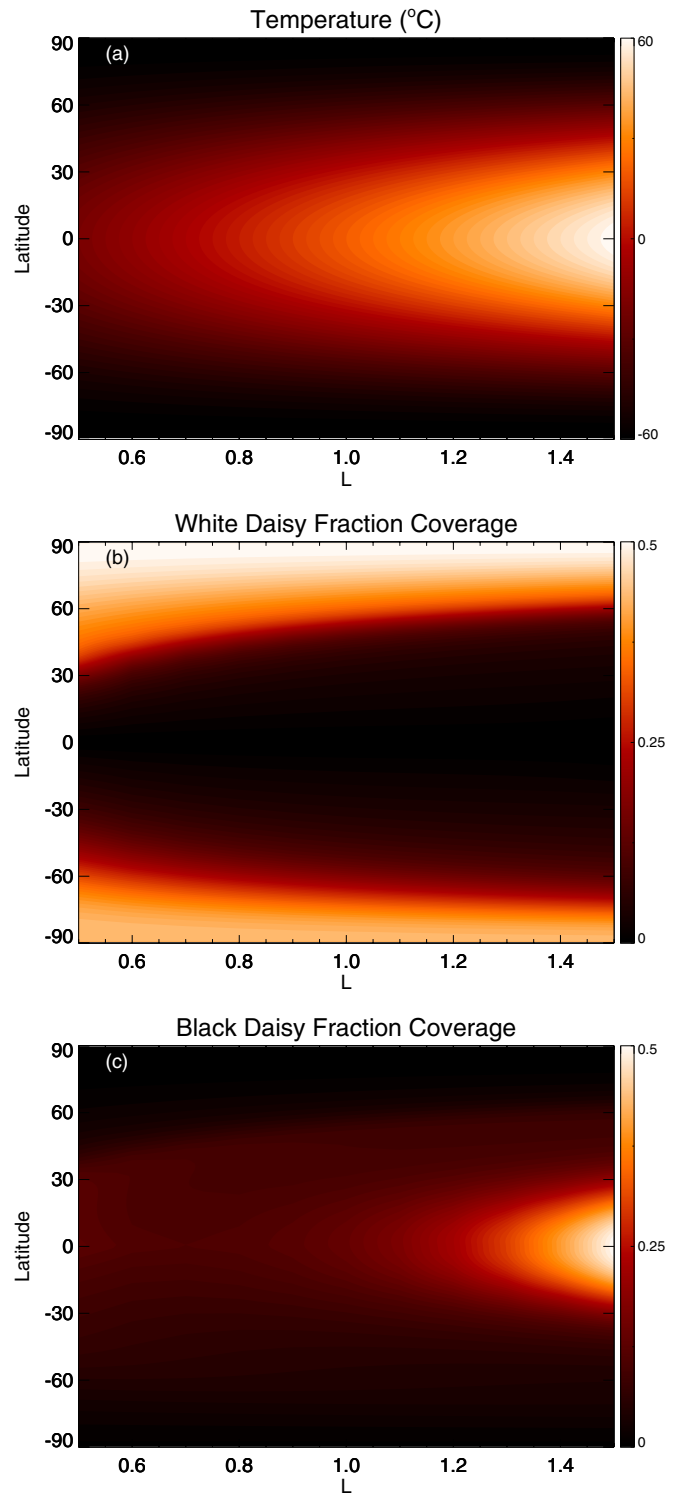


FIG. 4. (Color online) Contour plots of the stationary solutions for (a) $T(\theta)$, (b) white daisy population $\alpha_w(\theta)$, and (c) black daisy population $\alpha_b(\theta)$, in the plane (L, θ) using the profile (32) for $\kappa(\theta)$ and $g(T) = 1$.

$0 < k_\theta < 25$. These peculiar initial conditions are chosen in a way that the initial coverages correspond to the equilibrium coexistence solution and the temperature is kept in the range where the coexistence solution is stable. The function $\cos(k_\theta \theta)$

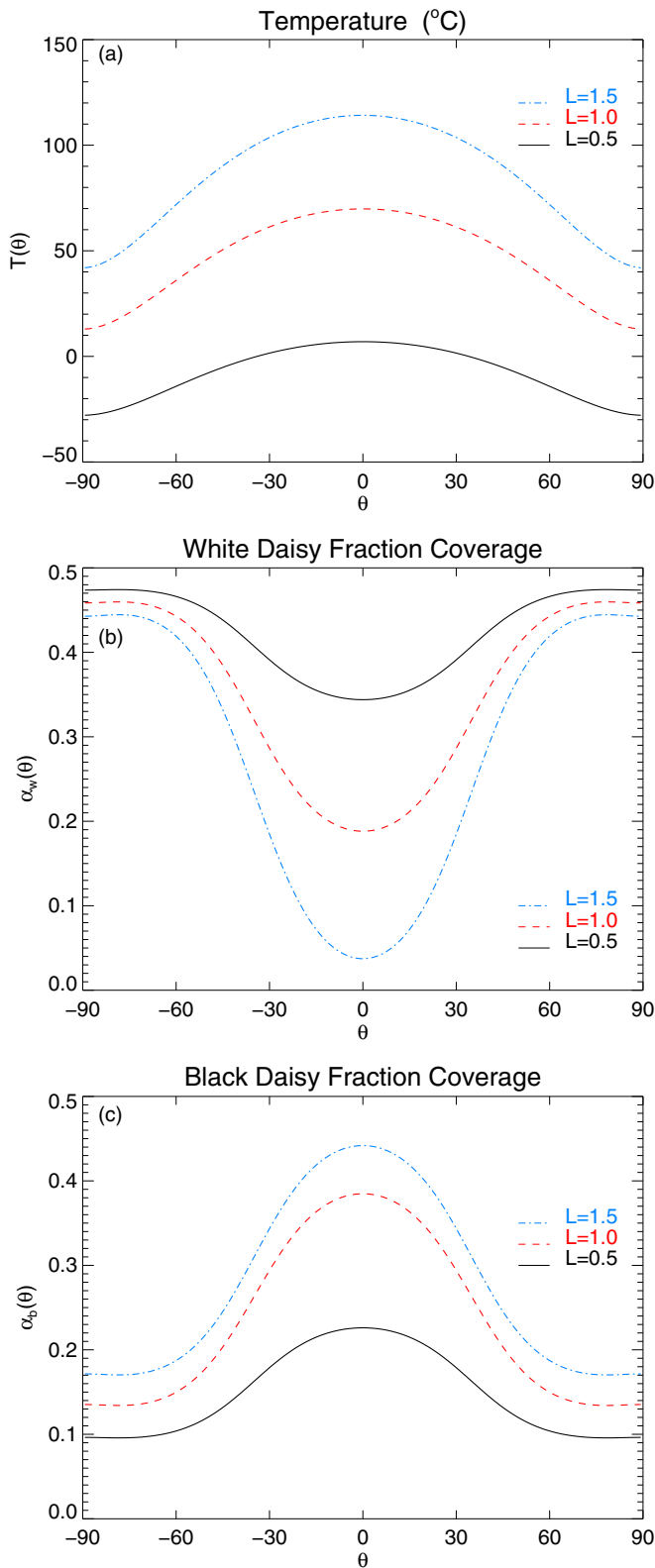


FIG. 5. (Color online) Stationary solutions for (a) $T(\theta)$, (b) white daisy population $\alpha_w(\theta)$, and (c) black daisy population $\alpha_b(\theta)$, as a function of latitude, by numerical solution of Eq. (9), using the profile (32) for $\kappa(\theta)$ and (13) for $g(T)$, and three different values of the parameter L .

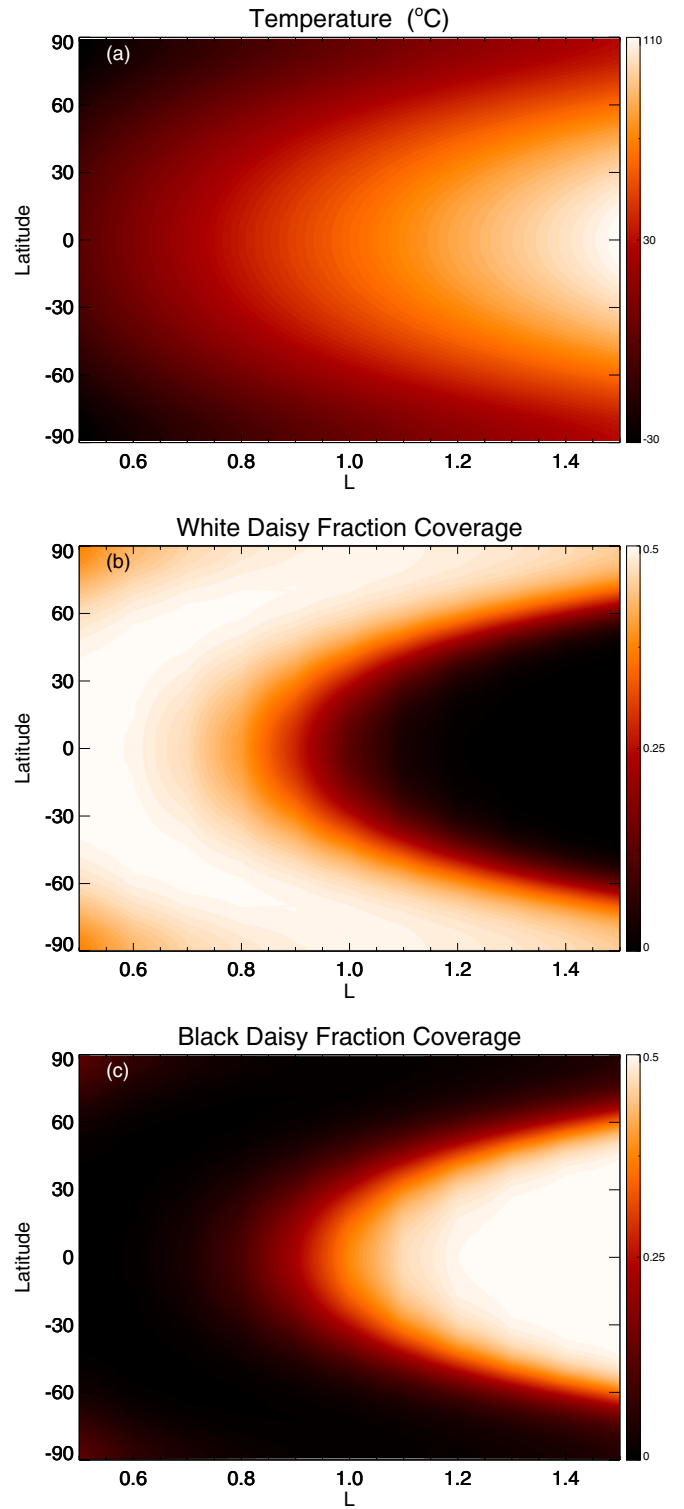


FIG. 6. (Color online) Contour plots of the stationary solutions for (a) $T(\theta)$, (b) white daisy population $\alpha_w(\theta)$, and (c) black daisy population $\alpha_b(\theta)$, in the plane (L, θ) using the profile (32) for $\kappa(\theta)$ and (13) for $g(T)$.

is introduced to study how initial temperature profile changes can affect the solutions and allows one to build up diagrams showing when multiple solutions take place. Figures 9, 10, and 11 show the temperature and daisy coverage solutions

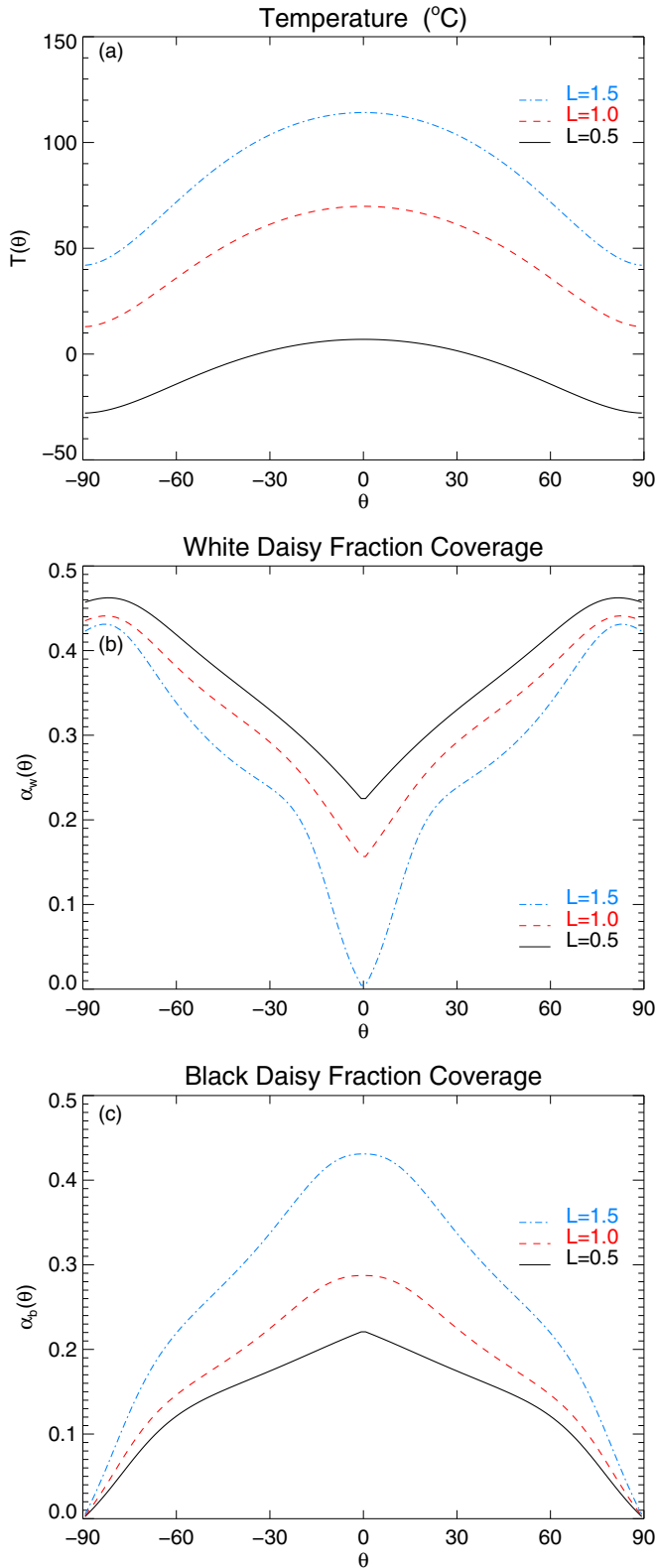


FIG. 7. (Color online) Same as Fig. 5, but with different initial values for vegetal coverages.

as functions of latitude and k_θ for three different values of L ($L = 0.5$ Fig. 9, $L = 1.0$ Fig. 10, and $L = 1.5$ Fig. 11). We remark that the temperature profile shape is almost not

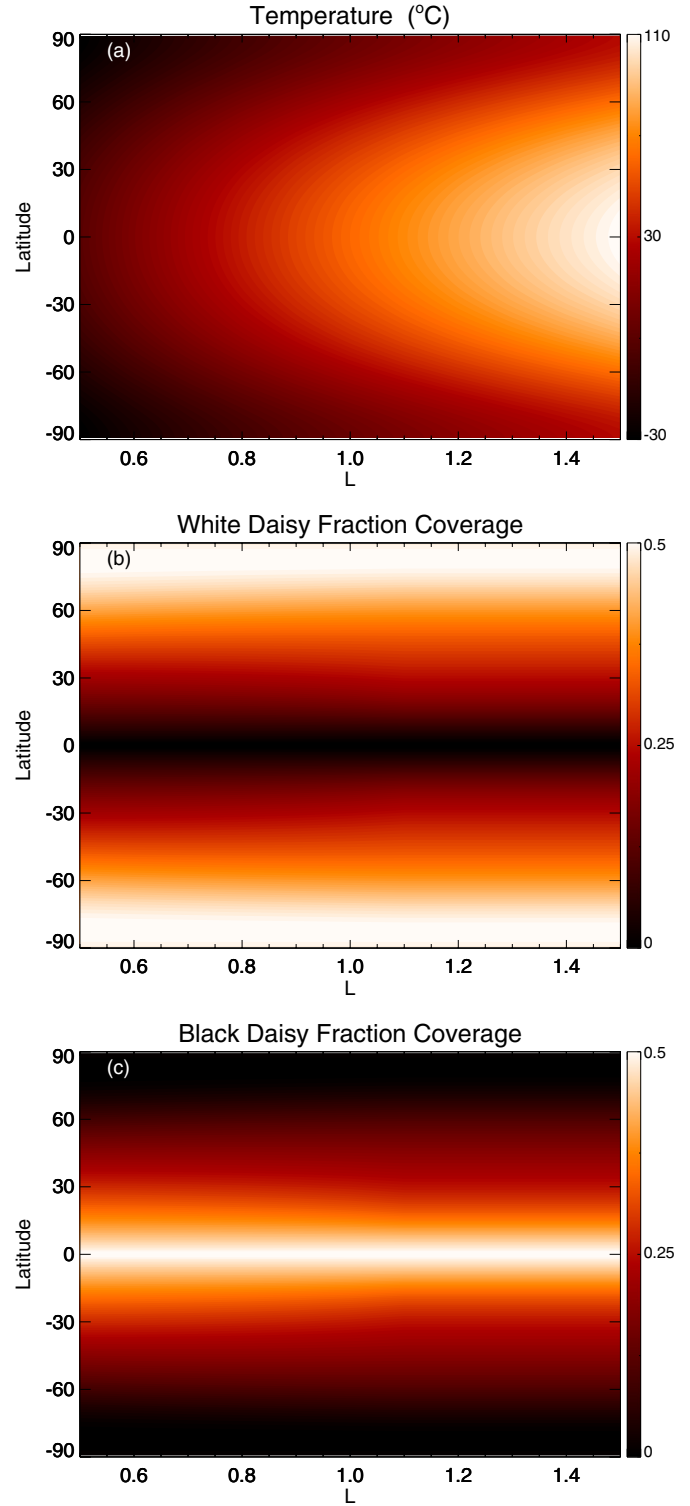


FIG. 8. (Color online) Same as Fig. 6, but with different initial values for vegetal coverages.

affected by the initial perturbation, since it does not vary substantially with k_θ and only an increase of temperature with L is found, as expected, without changes in the profile shape. On the other hand, the perturbations clearly affect the daisy coverages, which are found to significantly depend on k_θ . For $L = 0.5$ (Fig. 9), a striped pattern appears when $k_\theta \gtrsim 8$. This

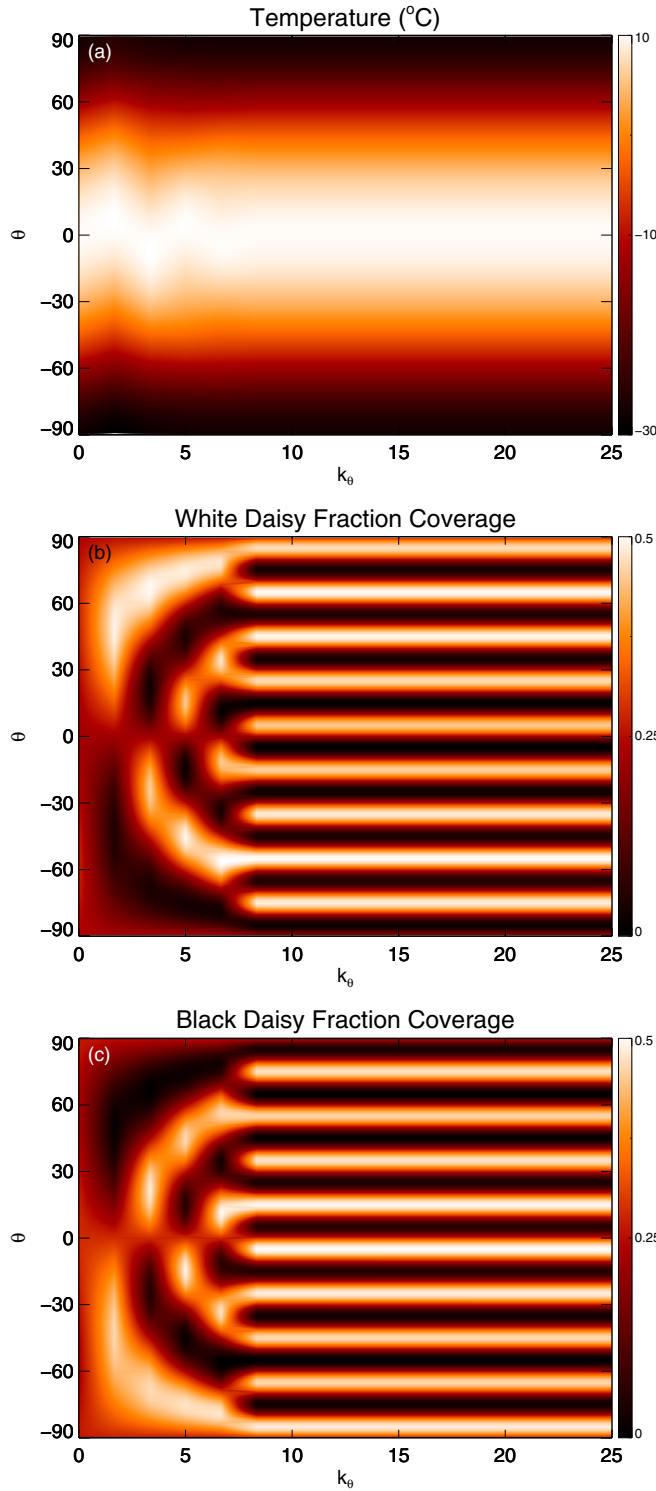


FIG. 9. (Color online) Contour plots of the stationary solutions for (a) $T(\theta)$, (b) white daisy population $\alpha_w(\theta)$, and (c) black daisy population $\alpha_b(\theta)$, in the plane (k, θ) for different initial conditions according to the value of k and fixing $L = 0.5$.

value of k_θ is in agreement with the value found through the stability analysis. The striped pattern is simultaneously observed in both the white and black daisy coverages, with the two populations covering almost the same area even for this low luminosity value. This effect is probably related

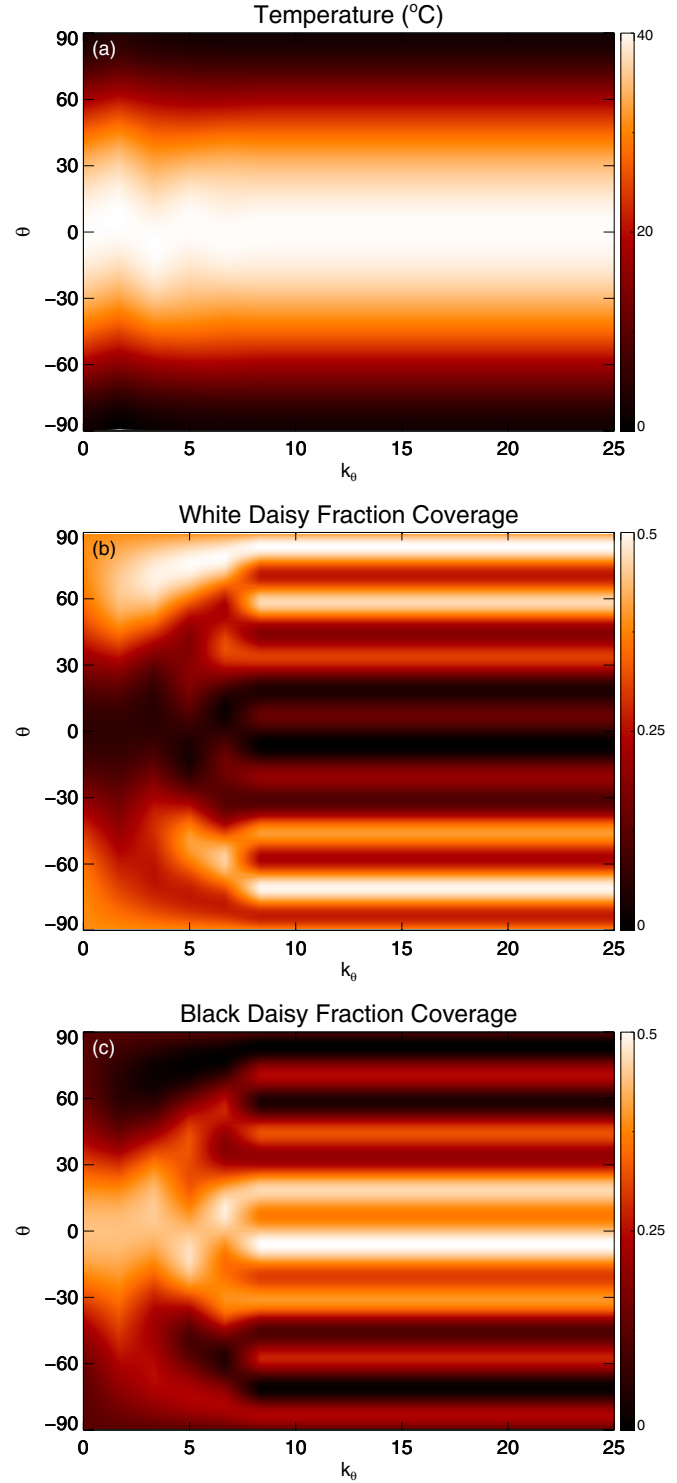


FIG. 10. (Color online) Contour plots of the stationary solutions for (a) $T(\theta)$, (b) white daisy population $\alpha_w(\theta)$, and (c) black daisy population $\alpha_b(\theta)$, in the plane (k, θ) for different initial conditions according to the value of k and fixing $L = 1.0$.

to the grayness function which regulates the temperature in a way that black daisies increase their growth rate. For $L = 1.0$, the same k_θ critical value is found and a large scale pattern is observed in addition to the stripes. More precisely, a clear separation between polar and equatorial regions is evident,

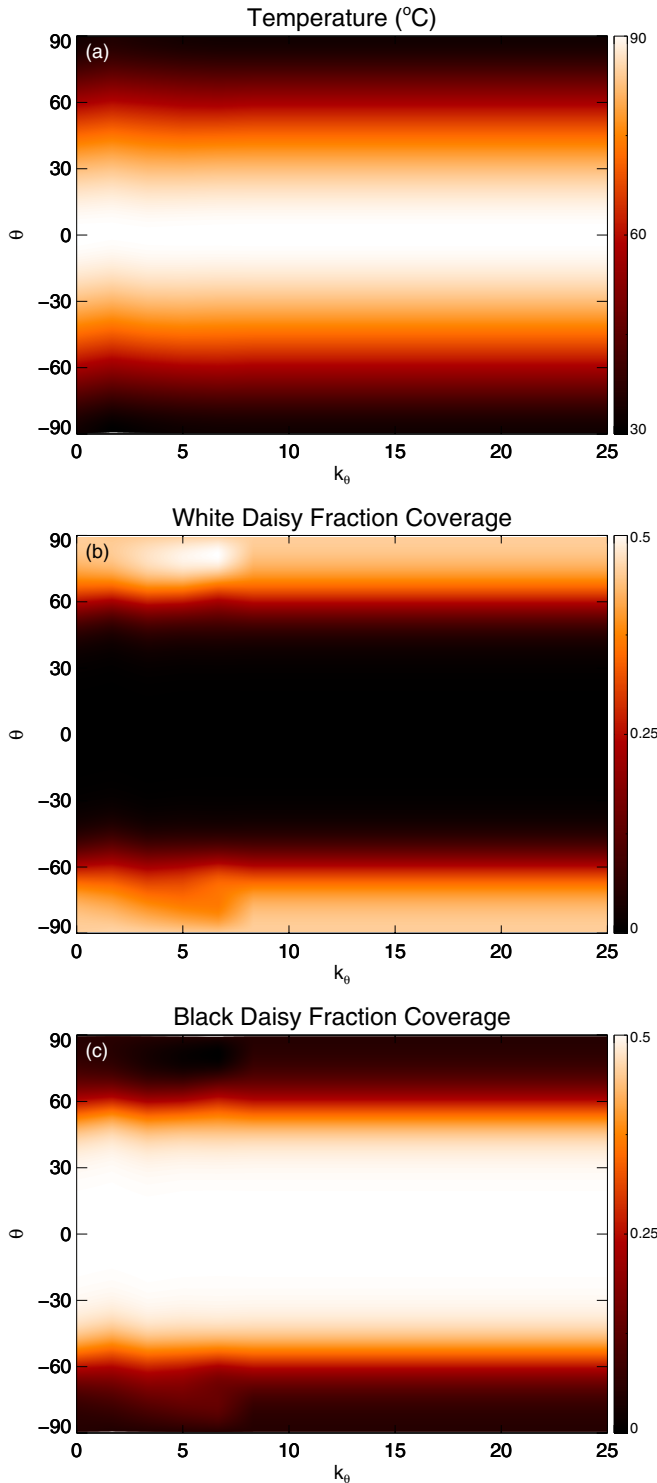


FIG. 11. (Color online) Contour plots of the stationary solutions for (a) $T(\theta)$, (b) white daisy population $\alpha_w(\theta)$, and (c) black daisy population $\alpha_b(\theta)$, in the plane (k, θ) for different initial conditions according to the value of k and fixing $L = 1.5$.

with white daisy stripes being dominant in the polar regions and black stripes at $|\theta| \lesssim 40^\circ$. For $L = 1.5$, the equilibrium solutions for the daisy coverages change again; only the large scale pattern survives, while no striped pattern occurs. The different behaviors observed for different L values are mainly attributable to the grayness function, whose effects are more pronounced for higher values of the temperature. On the other hand, the diffusion process produces a striped or continuous pattern for both white and black daisies according to the different values of the L parameter and to the different initial conditions when a small perturbation is introduced.

V. CONCLUSIONS

We investigated a modified Daisyworld model, where spatial dependency, variable heat diffusivity, and greenhouse effect are explicitly taken into account. The greenhouse effect has been modeled through a grayness function which modifies the blackbody radiative coefficient. We found that, at variance with previous results, the system is able to self-regulate even in the presence of values of the incident luminosity which are far from the current Sun-Earth conditions. In particular, the mutual exclusion of the two vegetation types is observed for particular initial conditions. Our investigation leads to the following conclusions.

(i) The diffusion process is able to destabilize the system and plays an important role in setting the symmetry with respect to the equator. The greenhouse effect, modeled through a grayness function, affects the temperature evolution and contributes to self-regulating the planet climate. Moreover, although it is seen that the grayness function does not destabilize the system, it modifies its stability properties.

(ii) The final equilibrium state is significantly dependent on the initial conditions. The initial conditions of daisy coverage influence the vegetation profiles although they do not significantly modify the temperature behavior. It was also found that, when small perturbations are present in the initial conditions of both temperature and daisy coverages, this gives rise to striped patterns for low-to-intermediate luminosity values when the perturbation wave number exceeds a threshold value. For high luminosities, the greenhouse effect leads to the disappearance of the striped patterns.

Of course the model can be further enriched by considering, for example, asymmetric initial conditions with respect to the equator. Moreover, extensions of the model to more realistic conditions, as for example the dependence of c_p and κ on temperature and more realistic greenhouse effects can also be introduced.

ACKNOWLEDGMENT

This work is partially supported by the Italian Ministry for Education and Research MIUR PRIN Grant No. 2012P2HRCR on “The active Sun and its effects on Space and Earth climate”.

[1] J. E. Lovelock, *Atm. Env.* **6**, 579 (1972); J. E. Lovelock and A. J. Watson, *Planet. Space Sci.* **30**, 795 (1982); J. E. Lovelock, *The Ages of Gaia: A Biography of Our Living Earth* (W. W. Norton

& Co., New York, 1995); *Philos. Trans. R. Soc., Ser. B* **338**, 383 (1992).

[2] A. J. Watson and J. E. Lovelock, *Tellus B* **35**, 284 (1983).

- [3] A. J. Wood, G. J. Ackland, J. G. Dyke, H. T. P. Williams, and T. M. Lenton, *Rev. Geophys.* **46**, RG1001 (2008).
- [4] S. De Gregorio, A. Pielke, and G. A. Dalu, *J. Nonlinear Sci.* **2**, 263 (1992); S. P. Harding and J. E. Lovelock, *J. Theor. Biol.* **182**, 109 (1996); C. Nevison, V. Gupta, and L. Klinger, *Tellus B* **51**, 806 (1999); S. L. Weber, *Climate Change* **48**, 465 (2001); T. M. Lenton and J. E. Lovelock, *J. Theor. Biol.* **206**, 109 (2000); *Tellus B* **53**, 288 (2001); J. D. Murray, *Mathematical Biology*, 2nd ed. (Springer, Berlin, 1993).
- [5] W. von Bloh, A. Block, and H. J. Schellnhuber, *Tellus B* **49**, 249 (1997).
- [6] G. J. Ackland, M. A. Clark, and T. M. Lenton, *J. Theor. Biol.* **223**, 39 (2003).
- [7] B. Adams, J. Carr, T. M. Lenton, and A. White, *J. Theor. Biol.* **223**, 505 (2003).
- [8] B. Adams and J. Carr, *Nonlinearity* **16**, 1339 (2003).
- [9] R. N. Carter and S. D. Prince, *Nature* **293**, 644 (1981).
- [10] W. D. Sellers, *J. Appl. Meteor.* **8**, 392 (1969)
- [11] M. Ghil, in *Theoretical Climate Dynamics: An Introduction*, Proceedings of the International School of Physics “E. Fermi,” Course LXXXVIII (Academic, London, 1985), pp. 347–402.